Luminescent Homoatomic Exciplexes in Dicyanoargentate(I) Ions Doped in Alkali Halide Crystals. 1. "Exciplex Tuning" by Site-Selective Excitation

Mohammad A. Omary[†] and Howard H. Patterson*

Contribution from the Department of Chemistry, University of Maine, Orono, Maine 04469

Received January 22, 1998

Abstract: The photoluminescence behavior of dicyanoargentate(I) ions doped in KCl host crystals has been studied. Several ultraviolet and visible emission bands are observed in this system. Each emission band becomes dominant at a characteristic excitation wavelength; that is, the energy of the emission can be tuned by site-selective spectroscopy. Both the experimental and the theoretical results suggest the formation of Ag−Ag-bonded excimers and exciplexes between adjacent $Ag(CN)_2^-$ ions in the host lattice. The experimental evidence includes the broadness, the absence of detailed structure, the large Stokes shifts, and the very low band energies of the luminescence bands. Meanwhile, ab initio calculations show that the LUMO is bonding with respect to Ag−Ag bonds while the HOMO is antibonding. Moreover, excited state extended Hückel calculations indicate the formation of exciplexes with shorter Ag−Ag distances, higher binding energies, and higher Ag−Ag overlap populations than the corresponding ground-state oligomers. The emission bands are assigned to different $*[Ag(CN)_2^-]_n$ luminescent exciplexes. Tuning of the emission over the 285−610-nm range has been achieved by site-selective excitation in a single $KCl:Ag(CN)_2^-$ crystal. The results in this work give rise to a new optical phenomenon we call "exciplex tuning".

Introduction

There has been increasing interest in coordination compounds with well-understood photophysical properties due to their roles in numerous potential applications. For example, metal diimine complexes, which have been studied extensively in the past 20 years,[1] have applications in solar energy conversion, supramolecular assemblies, photocatalysis, nonlinear optics, photonic devices, and photoluminescent probes of biological systems.[2−7] Meanwhile, interest in the photophysical and photochemical properties of d^{10} systems has been focused on coordination compounds of group 11 monovalent ions.[8] Historically, research in this field started with Cu(I) systems but has shifted in recent years to Au(I) systems. Interest in Cu(I) systems has been triggered by the rich luminescence properties of tetranuclear clusters of the type $Cu_4X_4L_4$ (X, halogen; L, amine or phosphine)[8a,9] which display interesting optical phenomena such as "luminescence thermochromism".[10] Another aspect of Cu(I) systems is their photochemical reactions which play a role in photocatalytic applications. For example, the $Cu(dpp)_2^+$ complex (dpp = 2,9-diphenyl-1,10-phenanthroline) has potential use as a photosensitizer for water splitting via energy- and electron-transfer pathways.[11] Gold(I) systems, on the other hand, have been the subject of numerous recent investigations aimed at understanding fundamental chemistry issues such as gold−gold interactions (aurophilic attraction) and supramolecular chemistry[12] as well as their potential applicability as optical sensors for volatile organic compounds (VOCs),[13] biosensors,[14] and as photocatalysts.[15]

Unlike other d^{10} systems, coordination compounds of Ag(I) have not been investigated extensively and only a few spectroscopic investigations have been reported for these compounds.[16−19] This has stimulated interest in our group to study Ag(I) coordination compounds. We have recently

[†] Present address: Department of Chemistry, Colby College, Waterville, Maine 04901.

(1) Balzani, V.; Moggi, L. *Coord. Chem. Rev.* **1990**, *97*, 313.
(2) Meyer, T. J. *Acc. Chem. Res.* **1989**, *22*, 163.
(3) Balzani, V.; Scandola, F. *Supramolecular Photochemistry*; Ellis Horwood: Chichester, UK, 1991.
(4) Pelizzetti, E.; Serpone, N. *Homogeneous and Heterogeneous Photocatalysis*; Pelizzetti, E., Serpone, N., Ed.; D. Riedel Publishing: Dordrecht, Holland, 1985.
(5) Cheng, L. T.; Tam, W; Eaton, D. F. *Organometallics* **1990**, *9*, 2856.
(6) Prasad, P. N.; Reinhardt, B. A. *Chem. Mater.* **1990**, *2*, 660.
(7) Friedman, A. E.; Chambron, J. C.; Sauvage, J. P.; Turro, N. J.; Barton, J. K. *J. Am. Chem. Soc.* **1990**, *112*, 4960.
(8) For reviews see: (a) Ford, P. C.; Vogler, A. *Acc. Chem. Res.* **1993**, *26*, 220. (b) Kutal, C. *Coord. Chem. Rev.* **1990**, *99*, 213. (c) Jansen, M. *Angew Chem.* **1987**, *99*, 1136; *Angew. Chem., Int. Ed. Engl.* **1987**, *26*, 1098.
(9) (a) Kyle, K. R.; Ryu, C. K.; DiBenedetto, J. A.; Ford, P. C. *J. Am Chem. Soc.* **1991**, *113*, 2954. (b) Kyle, K. R.; DiBenedetto, J. A.; Ford, P. C. *J. Chem. Soc., Chem. Commun.* **1989**, 714. (c) Kyle, K. R.; Ford, P. C. *J. Am Chem. Soc.* **1989**, *111*, 5005. (d) Kyle, K. R.; Palke, W. E.; Ford, P. C. *Coord. Chem. Rev.* **1990**, *97*, 35. (e) Døssing, A.; Ryu, C. K.; Kudo; S.; Ford, P. C. *J. Am Chem. Soc.* **1993**, *115*, 5132. (f) Ford, P. C. *Coord. Chem. Rev.* **1994**, *132*, 129. (g) Tran, D.; Ryu, C. K.; Ford, P. C. *Inorg Chem.* **1994**, *33*, 56. (h) Simon, J. A.; Palke, W. E.; Ford, P. C. *Inorg Chem.* **1996**, *35*, 6413. (i) Sabin, F.; Ryu, C. K.; Ford, P. C.; Vogler, A. *Inorg Chem.* **1992**, *31*, 1941.
(10) (a) De Ahna, H. D.; Hardt, H. D. *Z. Anorg. Allg. Chem.* **1972**, *387*, 61. (b) Hardt, H. D.; Gechnizdjani, H. *Z. Anorg. Allg. Chem.* **1973**, *397*, 23. (c) Hardt, H. D.; Pierre, A. *Z. Anorg. Allg. Chem.* **1973**, *402*, 107. (d) Hardt, H. D.; Pierre, A. *Inorg Chim. Acta* **1977**, *25*, L59. (e) Hardt, D. D.; Stoll, H. J. *Z. Anorg. Allg. Chem.* **1981**, *480*, 193. Hardt, D. D.; Stoll, H. J. *Z. Anorg. Allg. Chem.* **1981**, *480*, 199.
(11) Edel, A.; Marnot, P. A.; Sauvage, J. P. *Nouv. J. Chim.* **1984**, *8*, 495.
(12) Schmidbaur, H. *Chem. Soc. Rev.* **1995**, 391.
(13) Mansour, M. A.; Connick, W. B.; Lachicotte, R. J.; Gysling, H. J.; Eisenberg, R. *J. Am. Chem. Soc.* **1998**, *120*, 1329−1330.
(14) Blonder, R.; Levi, S., Tao, G.; Ben-Dov, I.; Willner, I. *J. Am. Chem. Soc.* **1997**, *119*, 10467−10478.
(15) Wolf, M. O.; Fox, M. A. *J. Am. Chem. Soc.* **1995**, *117*, 1845−1846.
(16) Fortin, D.; Drouin, M.; Turcotte, M.; Harvey, P. D. *J. Am. Chem. Soc.* **1997**, *119*, 531.
(17) Vogler, A.; Kunkely, H. *Chem. Phys. Lett.* **1989**, *158*, 74.
(18) Henary, M.; Zink, J. I. *Inorg Chem.* **1991**, *30*, 3111.
(19) Omary, M. A.; Patterson, H. H.; Shankle, G. *Mol. Cryst. Liq. Cryst.* **1996**, *284*, 399.

S0002-7863(98)00256-X CCC: $15.00 © 1998 American Chemical Society
Published on Web 07/24/1998

demonstrated the presence of ligand-unsupported Ag−Ag interactions (argentophilic attraction) in the mononuclear compound, $Tl[Ag(CN)_2]$.[20] The fact that Ag−Ag interactions in $Tl[Ag(CN)_2]$ and a few other examples[21−23] are ligand-unsupported indicates that *argentophilicity* is generally important in Ag(I) coordination compounds. The photoluminescence displayed by $Tl[Ag(CN)_2]$ has been explained in terms of excited-state Ag−Ag interactions leading to exciplex formation.[24] Exciplex formation in $Tl[Ag(CN)_2]$ is the first solid-state example for the formation of metal−metal-bonded exciplexes in coordination compounds.[24]

It has long been recognized that the formation of exciplexes is a well-known phenomenon in organic compounds.[25] On the other hand, inorganic exciplexes have been recognized only recently.[26] Recent reported examples involve coordination compounds of Pt(II),[27,28] Cu(I),[9c,29,30] Ru(II),[31] and Ir(III).[32] Cadmium and mercury form exciplexes with solvents.[33] Only a few examples are known in which exciplexes are metal−metal-bonded. Nagle et al. have reported exciplex formation in solutions of Pt(II) complexes in which Pt(II) is bonded with T1(I)[34] and Au(I).[35] Zink et al. have reported the formation of $*[Cu\text{-}Cu]^{2+}$ excimers[36a] and $*[Cu\text{-}Ag]^{2+}$ exciplexes[36b] in β''-alumina. The formation of the silver−silver-bonded exciplex, $*[Ag(CN)_2^-]_3$, in crystalline $Tl[Ag(CN)_2]$ has been described in our recent work.[24]

We report herein a new class of inorganic excimers and exciplexes in the $Ag(CN)_2^-$/KCl system in which the bonding occurs between the same type of metal atoms. Other examples of metal−metal-bonded exciplexes have the exciplex bond between different metal atoms.[34,35] In their classification of inorganic exciplexes, Horváth and Stevenson have categorized metal−metal-bonded exciplexes as one class.[26] The work herein suggests that this class should be subdivided into *homoatomic* and *heteroatomic* metal−metal-bonded exciplexes. Therefore, $*[Ag(CN)_2]_n$ are the first reported *homoatomic metal−metal-bonded exciplexes* in coordination compounds. The emission in the $Ag(CN)_2^-$/KCl system results from silver−silver-bonded excimers and exciplexes with a formula of $*[Ag(CN)_2^-]_n$. In this paper we refer to an excited state dimer as an "excimer" while excited-state trimers and longer oligomers are called "exciplexes".[37] The luminescence is *tuned* by selecting the excitation wavelength characteristic of each $*[Ag(CN)_2^-]_n$ emissive exciplex. These results are quite unprecedented in the photophysics of coordination compounds and thus give rise to a new optical phenomenon we call *exciplex tuning.* It is known that the tunability of the excited-state properties is an essential factor for the use of coordination compounds in most of the aforementioned applications.[2,38] The tunability of the excited states of dicyanoargentate(I) systems compares favorably with other systems that have been reported to display efficient tuning of their excited states.[38,39]

Experimental Section

Crystals of $KCl/Ag(CN)_2^-$ were grown by slow evaporation of aqueous solutions containing KCl and small amounts of $K[Ag(CN)_2]$. The silver content was determined by atomic absorption spectroscopy using a Varian SpectrAA-20 spectrophotometer with an air−acetylene flame and a Ag analytical lamp operating at 328.1 nm. The standards for the atomic absorption analysis were prepared using Aldrich 1000 ppm Ag standard in 1% HNO_3.

Photoluminescence spectra were recorded with a Model Quanta-Master-1046 fluorescence spectrophotometer from Photon Technology International, PTI. The instrument is equipped with two excitation monochromators and a 75-W xenon lamp. All luminescence spectra were recorded at liquid nitrogen temperature for a single crystal using a Model LT-3-110 Heli-Tran cryogenic liquid transfer system. Correction of the excitation spectra for the lamp background was carried out using the quantum counter rhodamine B. Lifetime measurements were carried out with a LaserStrobe system from PTI equipped with a nitrogen laser, a dye laser, a frequency doubler, and a gated microsecond detector for the microsecond time domain. Some measurements were carried out with a QuantaMaster-2 system utilizing a microsecond Xe flash lamp. A Beckman Model DU-640 spectrophotometer was used for UV−vis absorption spectra. An aqueous solution of $K[Ag(CN)_2]$ was used for absorption measurements. The solution was placed in a

(20) Omary, M. A.; Webb, T. R.; Assefa, Z.; Shankle, G. E.; Patterson, H. H. *Inorg. Chem.* **1998**, *37*, 1380.
(21) Singh, K; Long, J. R.; Stavropoulos, P. *J. Am. Chem. Soc.* **1997**, *119*, 2942.
(22) Kim, Y.; Seff, K. *J. Am. Chem. Soc.* **1977**, *99*, 7055. Kim, Y.; Seff, K. *J. Am. Chem. Soc.* **1978**, *100*, 175.
(23) Eastland, G. W.; Mazid, M. A.; Russell, D. R.; Symons, M. C. R. *J. Chem. Soc., Dalton Trans.* **1980**, 1682.
(24) Omary, M. A.; Patterson, H. H. *Inorg Chem.* **1998**, *37*, 1060.
(25) (a) Lowry, T. H.; Schuller-Richardson, K. *Mechanism and Theory in Organic Chemistry*; Harper & Row: New York, 1981; pp 919−925. (b) Turro, N. J. *Modern Molecular Photochemistry*; Benjamin/Cummings: Menlo Park, CA, 1978; pp l35−146. (c) Lamola, A. A. In *Energy Transfer and Organic Photochemistry*; Lamola, A. A., Turro, N. J., Eds.; Wiley-Interscience: New York, 1969; pp 54−60. (d) *The exciplex*; Gordon, M., Ware, W. R., Eds; Academic Press: New York, 1975. (e) Kopecky, J. *Organic Photochemistry: A Visual Approach*; VCH: New York, 1991; pp 38−40. (f) Michl, J.; Bonačić-Koutecký, V. *Electronic Aspects of Organic Photochemistry*; Wiley: New York, 1990; pp 274−286.
(26) For a recent review see: Horváth, A.; Stevenson, K. L. *Coord. Chem. Rev.* **1996**, *153*, 57.
(27) Bailey, J. A.; Hill, M. G.; Marsh, R. E.; Miskowski, V. M.; Schaefer, W. P.; Gray, H. B. *Inorg Chem.* **1995**, *34*, 4591. Miskowski, V. M.; Houlding, V. H. *Inorg Chem.* **1989**, *28*, 1529.
(28) (a) Chan, C.-W.; Lai, T.-F.; Che, C.-M.; Peng, S.-M. *J. Am. Chem. Soc.* **1993**, *115*, 11379. (b) Kunkely, H.; Vogler, A. *J. Am. Chem. Soc.* **1990**, *112*, 5625.
(29) Stevenson, K. L.; Dhawale, R. S.; Horváth, A.; Horváth, O. *J. Phys. Chem. A* **1997**, *101*, 3670. Stevenson, K. L.; Knorr, D. W.; Horváth, A. *Inorg. Chem.* **1996**, *35*, 835. Horváth, A.; Wood, C. E.; Stevenson, K. L. *Inorg. Chem.* **1994**, *33*, 5351. Horváth, A.; Wood, C. E.; Stevenson, K. L. *J. Phys. Chem.* **1994**, *98*, 6490. Horváth, A.; Stevenson, K. L. *Inorg Chem.* **1993**, *32*, 2225.
(30) Stacy, E. M.; McMillin, D. R. *Inorg Chem.* **1990**, *29*, 393. Palmer, C. E. A.; McMillin, D. R.; Kirmaier, C.; Holten, D. *Inorg Chem.* **1987**, *26*, 3167.
(31) Ayala, N. P.; Demas, J. N.; DeGraff, B. A. *J. Phys. Chem.* **1989**, *93*, 4104. Ayala, N. P.; Demas, J. N.; DeGraff, B. A. *J. Am. Chem. Soc.* **1988**, *110*, 1523.
(32) Ayala, N. P.; Flynn, C. M., Jr.; Sacksteder, L.; Demas, J. N.; DeGraff, B. A. *J. Am. Chem. Soc.* **1990**, *112*, 3839.
(33) Yamamoto, S.; Doi, M. *J. Chem. Soc., Faraday Trans.* **1997**, *93*, 1309. Takahashi, O.; Sotowa, C.; Saito, K.; Ahmed, O.; Yamamoto, S. *J. Chem. Soc., Faraday Trans.* **1995**, *91*, 3795.
(34) (a) Clodfelter, S. A.; Doede, T. M.; Brennan, B. A.; Nagle, J. K.; Bender, D. P.; Turner, W. A.; LaPunzia, P. M. *J. Am. Chem. Soc.* **1994**, *116*, 11379. (b) Nagle, J. K.; Brennan, B. A. J. *Am. Chem. Soc.* **1988**, *110*, 5931.
(35) (a) Nagle, J. K. Luminescent Excimers and Exciplexes Formed from Pt(II) Monomer and Dimer Compounds: Relativistically-Influenced Metal-Metal Interactions. Lecture presented in the 12th International Symposium on Photochemistry and Photophysics of Coordination Compounds. Saint Michael's College, Vermont, 1997. (b) Pettijohn, C. N.; Chuong, B.; Nagle, J. K.; Vogler, A. Luminescent Excimers and Exciplexes of Pt(II) Compounds. *Coord. Chem. Rev.*, in press.
(36) (a) Hollingsworth, G.; Barrie, J. D.; Dunn, B.; Zink, J. I. *J. Am. Chem. Soc.* **1988**, *110*, 6569. (b) Barrie, J. D.; Dunn, B.; Zink, J. I. *J. Am. Chem. Soc.* **1990**, *112*, 5701.
(37) The term "excimer" was first used in organic compounds to indicate excited state dimers of the same species ($*A_2$). When similar dimers were discovered later but between two different atoms (*AB), these dimers were called "exciplexes" to distinguish them from the first type. The word "exciplex" is used to describe an excited state complex. We cannot use the word "excimer" herein because $[Ag(CN)_2^-]_n$ aggregations are not restricted to dimers and thus we elected to use the word "exciplex" because it is more general.
(38) Cummings, S. D.; Eisenberg, R. *J. Am. Chem. Soc.* **1996**, *118*, 1949.
(39) Yersin, H.; Gliemann, G. *Ann. N. Y. Acad. Sci.* **1978**, *313*, 539. Gliemann, G.; Yersin, H. *Struct. Bond.* **1985**, *62*, 87 and references therein.

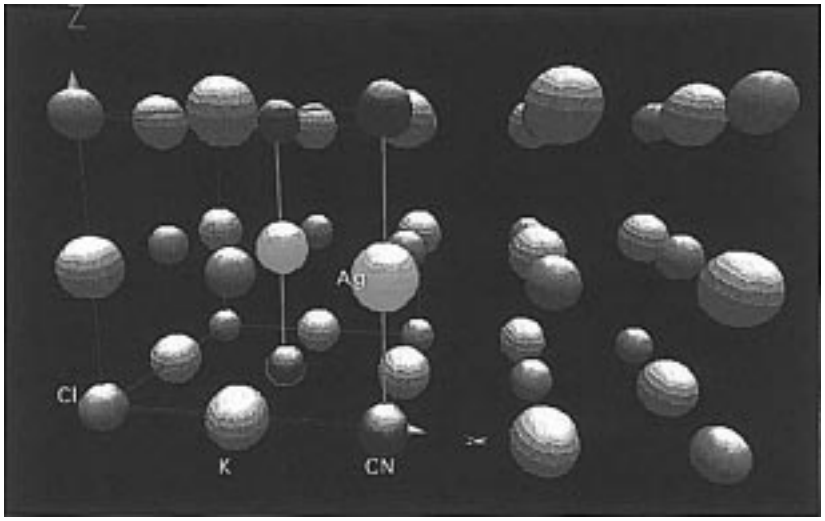

Figure 1. Structure of a unit cell of KCl with a defect created by doping two adjacent $Ag(CN)_2^-$ ions. In the defect, the Ag^+ and CN^- ions are shown to occupy the K^+ and Cl^- sites, respectively.

supracell quartz capillary tube and inserted into a liquid nitrogen Dewar flask with a quartz window. Fourier transform infrared (FTIR) spectra were obtained using a Bio-Rad Digilab FTS-60 spectrometer equipped with a microscope accessory and a liquid nitrogen cooled detector. This setup allows for measuring the FTIR spectra of single crystals using the reflectance mode.

Computational Details

Extended Hückel molecular orbital calculations were performed using the FORTICON8 program (QCMP011). Relativistic parameters were used for all atoms and the details are described elsewhere.[19] The calculations were carried out for a monomer, dimer, and trimer of $Ag(CN)_2^-$ ions in a KCl crystal lattice. The dopant $Ag(CN)_2^-$ ions are distributed in the KCl lattice creating crystal defects in which the Ag^+ and CN^- ions replace K^+ and Cl^- ions, respectively. Figure 1 shows the structure of a defect in the KCl lattice caused by two adjacent $Ag(CN)_2^-$ ions aligned in an eclipsed ($D_{\infty h}$) configuration. The dimer can also be arranged in two other configurations not shown in Figure 1, perpendicular (C_{2v}) and offset-eclipsed (C_{2v}). Chart 1 shows the three possible configurations of the dimer. All neighboring ions for each Ag^+ ion in the same layer were accounted for in the calculations. For example, a monomer defect was modeled by a layer containing a Ag^+ ion with four neighboring Cl^- ions separated by 3.19 Å and four neighboring K^+ ions separated by 4.50 Å.[40] The two cyanide ligands were placed directly above and below the Ag^+ ion (in the next layers). Ground- and excited-state extended Hückel calculations were also carried out for isolated monomer, dimer, trimer, and pentamer units of $Ag(CN)_2^-$ using the same program. These calculations were carried out for eclipsed ($D_{\infty h}$) and staggered (D_{2h}) dimer models. For the trimer models, the array of Ag atoms has a linear arrangement (*trans*-, $D_{\infty h}$) in one model and an angular arrangement (*cis*-, C_{2v}) in the other. The array of Ag atoms has a square-planar (D_{4h}) arrangement in the pentamer.

Chart 1

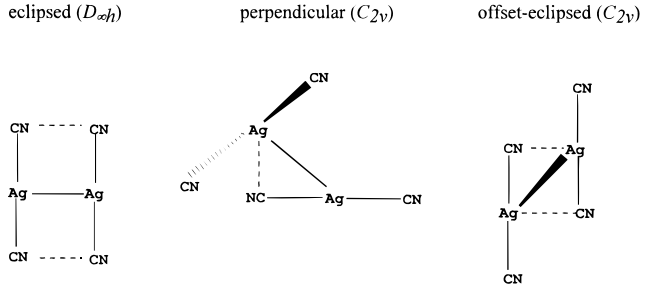

Restricted Hartree−Fock ab initio calculations were carried out using the STO-3G basis set available in SPARTAN (Version 4.1.1, Wavefunction Incorporated, Irvine, CA) to generate the HOMO and LUMO surfaces of $[Ag(CN)_2^-]_n$ oligomers. Density functional calculations on the BECKE3LYP level were carried out to calculate the energies of different configurations of the $[Ag(CN)_2^-]_2$ dimer. The LANL2DZ split-valence basis set that utilizes the Hay−Wadt effective core potential for silver was used in the density functional calculations. These calculations were carried out using Cerius[2] (Release 3.0, Molecular Simulations Inc.).

Results and Discussion

1. Atomic Absorption and FTIR Data. Atomic absorption analysis of the studied KCl mixed crystals gave rise to a silver content of 1.6% (by weight). The number of Ag^+ ions replacing K^+ ions determines the extent of Ag−Ag interactions. Despite the low silver content in the mixed crystals, Ag−Ag interactions are expected to be present for two reasons. First, the statistical probability of Ag^+ ions to be adjacent is relatively high due to the large number of neighboring K^+ sites. For a given K^+ ion there are 12 other next-neighbor K^+ ions in the unit cell (four in the same layer and four in each of the layers directly above and below. Second, our recent MO calculations indicate that $Ag(CN)_2^-$ ions have a thermodynamically driven tendency to aggregate.[20] Details of the statistical distribution analysis are discussed below.

Figure 2 shows the cyanide region of the FTIR spectrum of a single crystal of KCl/$Ag(CN)_2^-$. There are at least four resolved peaks in this infrared region. The presence of more than one peak in the ν_{C-N} region indicates the presence of more than one site for the $Ag(CN)_2^-$ ions in the mixed crystal. This is likely due to crystal defects in the KCl host crystal created by the doped $Ag(CN)_2^-$ ions present in different aggregations (i.e., $[Ag(CN)_2^-]_n$) and different orientations. Infrared spectra for solid $K[Ag(CN)_2]$ (mineral oil mulls) have been reported previously and show only one strong band in the ν_{C-N} region.[41] The possibility of combination bands is slim due to the low

(40) On the basis of the values of the ionic radii of hexacoordinated K^+ and Cl^-: Shannon, R. D. *Acta Crystallogr.* **1976**, *A32*, 751.

(41) Chadwick, B. M.; Frankiss, S. G. *J. Mol. Struct.* **1968**, *2*, 281. Bottger, G. L. *Spectrochim. Acta* **1968**, *24A*, 1821. Hildago, A.; Mathieu, J. P. *Compt. Rend.* **1959**, *249*, 233. Jones, L. H. *J. Chem. Phys.* **1957**, *26*, 1578.

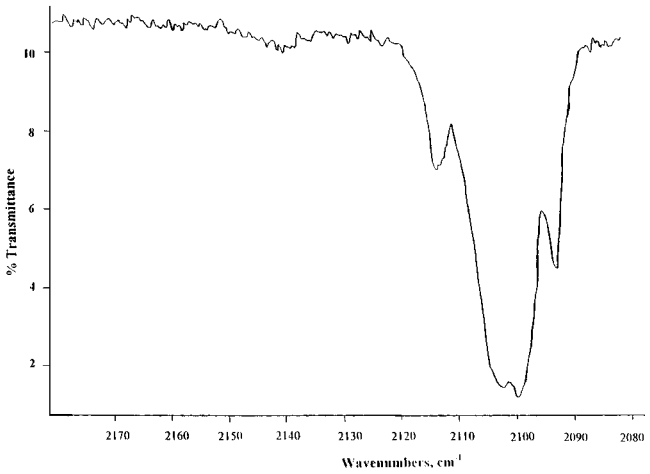

Figure 2. Infrared spectrum of a single crystal of $KAg(CN)_2$/KCl at room temperature in the region of the cyanide stretching frequency.

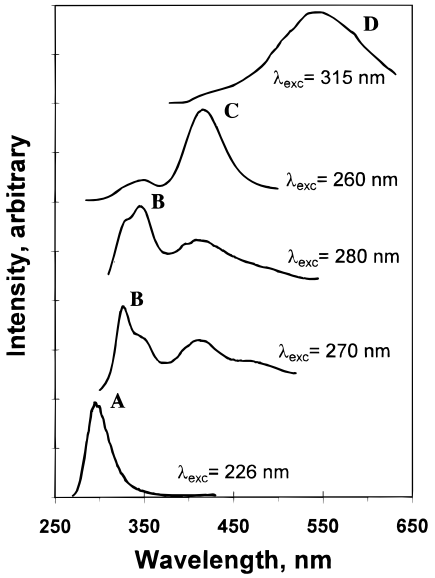

Figure 3. Exciplex tuning by site-selective excitation: emission spectra of a $KAg(CN)_2$/KCl crystal at 77 K with different excitation wavelengths. Intensities are not comparable between different spectra.

doping level of $Ag(CN)_2^-$ in KCl. By virtue of the microscope setup of our FTIR spectrometer, the infrared spectrum in Figure 2 is for the same intact single crystal used for the optical studies in this work which allows good correlation with the luminescence spectra.

2. Photoluminescence Spectra. Figure 3 shows the emission spectra of $Ag(CN)_2^-$/KCl single crystals. The emission profile is strongly dependent on the excitation wavelength. Emission peaks at ca. 295, 327, 345, 417, and 548 nm are observed upon excitation with the indicated wavelengths. We categorize four luminescence bands throughout this paper: A, B, C, and D, as labeled in Figure 3. The emissions at 327 and 345 nm are given the same label because they strongly overlap with each other and have similar excitation spectra.

Since the luminescence of d^{10} systems has a demonstrated sensitivity to metal−metal interactions, different emissions are expected to occur from various Ag centers in the doped crystals (monomers, dimers, trimers, etc.). Therefore, the emission bands in Figure 3 are likely due to the presence of different aggregations of the $Ag(CN)_2^-$ ions in the KCl host lattice. This is in agreement with the above prediction based on the infrared data.

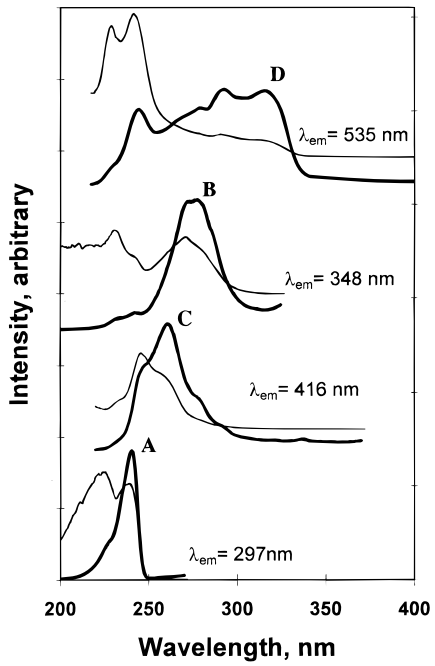

Figure 4. Corrected (thin lines) and uncorrected (thick lines) excitation spectra of a $KAg(CN)_2$/KCl crystal at 77 K monitoring the emissions at wavelengths corresponding to the emission maxima of bands A−D in Figure 3. Intensities are not comparable between different spectra.

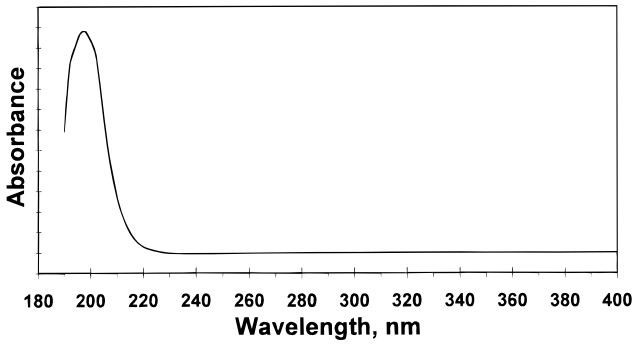

Figure 5. Absorption spectrum of an aqueous solution of $KAg(CN)_2$ at room temperature. The spectrum is the same at 77 K as at room temperature.

Excitation spectra have been obtained for each emission band. Figure 4 shows the excitation spectra of $Ag(CN)_2^-$/KCl single crystals with the emission monitored at wavelengths that correspond to each of the emission bands A−D, vide infra. Figure 4 shows that each emission band is associated with a different excitation peak. Therefore, the different emission bands are resolved by site-selective excitation. Individual peaks within different excitation bands are most likely due to different orientations of $Ag(CN)_2^-$ units in the crystal lattice.

Figure 5 shows the room temperature absorption spectrum of an aqueous solution of $K[Ag(CN)_2]$. Figure 5 shows that an absorption peak occurs at 196 nm ($\sim 51 \times 10^3$ cm^{-1}). The position of this absorption peak did not shift even at liquid nitrogen temperature. Cooling has only resulted in a higher extinction coefficient. Similar absorption data were reported for aqueous $K[Ag(CN)_2]$ by Mason.[42] The absorption peak (50.70×10^3 cm^{-1}; $\epsilon = 2.1 \times 10^4$ L mol^{-1} cm^{-1} at room temperature) has been characterized as a metal-to-ligand charge transfer (MLCT) band.[42] The absorption in Figure 5 is, therefore, assigned to a Laporte-allowed charge-transfer transi-

(42) Mason, W. R. *J. Am. Chem. Soc.* **1973**, *95*, 3573.

Table 1. Frontier Orbital Energies for $[Ag(CN)_2^-]_n$ Species Doped in KCl from Extended Hückel Calculations[a]

species	undoped $[Ag(CN)_2^-]$	monomer/ KCl	dimer/ KCl	trimer/ KCl
HOMO, eV	−11.22	−10.52	−10.51	−10.51
LUMO, eV	−6.01	−5.17	−5.24	−5.27
HOMO−LUMO gap, eV	5.21	5.35	5.27	5.23
total energy, eV	−498.11	−1032.26	−1797.39	−2562.51

[a] The calculations have been carried out for eclipsed configurations of the dimer and trimer only.

tion from the d^{10} orbitals of Ag(I) to the empty π^* orbitals of CN^-. Surprisingly, the excitation bands in Figure 4 are largely red-shifted from the absorption band of an aqueous solution of $K[Ag(CN)_2]$. The excitation peaks of the $KCl/Ag(CN)_2^-$ mixed crystals shown in Figure 4 are red-shifted by as much as 23×10^3 cm^{-1} from the energy of the absorption peak of aqueous $K[Ag(CN)_2]$. Silver−silver interactions are likely responsible for such a large shift. A similar conclusion has been reached in interpreting the low energies for the excitation bands in $Tl[Ag(CN)_2]$ which has Ag−Ag distances as short as 3.11 Å.[24] The excitation spectra of $Tl[Ag(CN)_2]$ are red-shifted by as much as 19×10^3 cm^{-1} from the absorption bands of $(n\text{-}Bu)_4N[Ag(CN)_2]$ in which no Ag−Ag interactions are present.[42]

3. Electronic Structure Calculations. In order to understand the nature of Ag−Ag interactions, we have carried out extended Hückel calculations for monomer, dimer, and trimer units of dicyanoargentate(I) doped in the KCl lattice as described in the Computational Details section. The calculations were also carried out for a free (undoped) $Ag(CN)_2^-$ ion to study the effect of the doping. Table 1 summarizes the results of these calculations. Table 1 shows that the highest occupied molecular orbital (HOMO) and the lowest unoccupied molecular orbital (LUMO) are both destabilized as a result of doping $Ag(CN)_2^-$ in KCl. This can be ascribed to the increased ligand field due to the chloride ions which act as ligands to Ag(I) in the doped crystals. Table 1 also shows that the HOMO−LUMO gap for $Ag(CN)_2^-$ increases upon doping the monomer in KCl. This suggests that the excitation energy of the monomer should increase in the KCl environment. Since all excitation bands for the doped crystals (Figure 4) have lower energies than the absorption band of free $Ag(CN)_2^-$ (Figure 5), none of the excitation bands is assigned to the monomer. These results suggest that the $Ag(CN)_2^-$ monomer does not luminesce and that Ag−Ag interactions must exist in order to observe luminescence. Energy-transfer pathways from the excited states of monomer sites to the excited states of oligomer sites in the KCl lattice are thus responsible for the observed luminescence.

Table 1 shows that the HOMO−LUMO gap decreases in the direction of monomer → dimer → trimer of doped ions. Ground-state Ag−Ag interactions are thus present in the $Ag(CN)_2^-$-doped KCl crystals. However, the decrease in the HOMO−LUMO gap in Table 1 is very small and cannot explain the low energies of the luminescence bands in Figures 3 and 4. This result is not surprising since the Ag−Ag separation of 4.5 Å in the doped crystals is significantly longer than the summed van der Waals radii of two Ag atoms (3.40 Å). Ground-state Ag−Ag interactions are too weak to cause the low energies of the luminescence bands of the studied crystals. This is unlike Au−Au interactions which can be significant in the ground state due to the relativistic effects which are much greater in Au than Ag. A study by Cotton et al. showed that little or no bonding takes place between Ag(I) centers in the ground state even in compounds with a Ag−Ag distance as short as 2.70 Å.[43] Excited-state Ag−Ag interactions are, therefore, expected to be the reason behind the very low energies of the luminescence bands of the $KCl/Ag(CN)_2^-$ crystals shown in Figures 3 and 4.

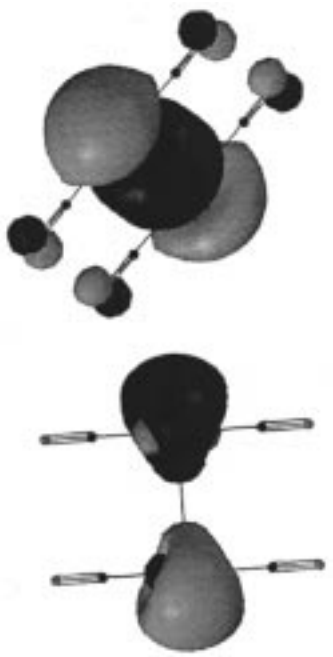

Figure 6. Surfaces of the HOMO (top) and LUMO (bottom) orbitals of $[Ag(CN)_2^-]_2$ (eclipsed configuration) as plotted from Hartree−Fock ab initio calculations. Note the Ag−Ag antibonding character of the HOMO and the Ag−Ag bonding character of the LUMO. Note that for the LUMO the interaction is primarily between the $5p_z$ atomic orbitals of the two Ag atoms (the *z* axis passes through both Ag atoms).

To test the possibility of excited-state Ag−Ag interactions, we have performed ab initio and extended Hückel calculations for oligomeric units of $Ag(CN)_2^-$. Since the effect of varying the Ag−Ag distance is sought, these calculations have been carried out for free $[Ag(CN)_2^-]_n$ oligomers instead of ones doped in the KCl lattice. Both calculation methods suggest exciplex formation in the $[Ag(CN)_2^-]_n$ models. Figure 6 shows the surfaces of the HOMO and LUMO orbitals for the eclipsed configuration of $[Ag(CN)_2^-]_2$, respectively. These surfaces are plotted from the output of our Hartree−Fock ab initio calculations. Figure 6 shows that the HOMO has an antibonding character with respect to Ag−Ag bonding while the LUMO has a Ag−Ag bonding character. A similar result was obtained for the staggered conformer. The same can be said about the Ag−Ag bonding characters of the frontier orbitals in the $[Ag(CN)_2^-]_3$ trimer and the $[Ag(CN)_2^-]_5$ pentamer (details are available in the Supporting Information).

Our ab initio calculations thus clearly indicate that for all studied aggregations of $Ag(CN)_2^-$ the HOMO is always antibonding while the LUMO is bonding with respect to Ag−Ag regardless of the configuration. As a consequence, a net bonding is expected to result in each species upon one-electron excitation from the HOMO to the LUMO. This leads to a formal increase of the Ag−Ag bond order in the excited state by 1, 0.5, and 0.25 unit for the dimer, trimer, and the pentamer, respectively. These results satisfy the ground-state requirements for exciplex formation.

Extended Hückel calculations yielded similar qualitative results to the ab initio calculations with regard to the bonding

(43) Cotton, F. A.; Feng, X.; Matusz, M.; Poli, R. *J. Am. Chem. Soc.* **1988**, *110*, 7077.

Table 2. Summary of the Results of Extended Hückel Calculations for the Ground and Excited States of Oligomeric Species of Dicyanoargentate(I)

species[a]	[S]	$[S]_2$ (*ec*)	$*[S]_2$ (*ec*)	$[S]_2$ (*st*)	$*[S]_2$ (*st*)	$[S]_3$ (*T1, ec*)	$*[S]_3$ (*T1, ec*)	$[S]_3$ (*T1, st*)	$*[S]_3$ (*T1, st*)	$[S]_3$ (*T1, ec*)	$*[S]_3$ (*T1, ec*)
Ag−Ag eq. diet., Å	8.00[d]	3.58	3.00	2.88	2.39	3.49	3.09	2.79	2.46	3.54	3.15
binding energy, eV	0.00	0.13	1.12	0.22	1.32	0.33	1.47	0.61	2.00	0.29	1.14
H−L gap,[b] eV	4.95	4.37	3.98	4.28	4.13	4.00	3.55	3.73	3.46	4.17	3.83
O.P.[c] (Ag−Ag)	0.000	0.003	0.034	0.069	0.089	−0.008	0.027	0.039	0.079	0.003	0.048

[a] Notation: $[S]_n$, $[Ag(CN)_2^-]_n$; $*[S]_n$, excimer/exciplex; *ec*, eclipsed; *st*, staggered; *T1*, linear trimer (*trans*-); *T2*, angular trimer (*cis*-). See Charts 1 and 2 for dimer and trimer configurations. [b] HOMO−LUMO gap. [c] O.P. = Overlap population. Values listed for bonds with the central silver atom. [d] Isolated ions are considered at a Ag−Ag distance with a total energy that does not change (within 0.01 eV) at longer distances. See plateau in Figure 7.

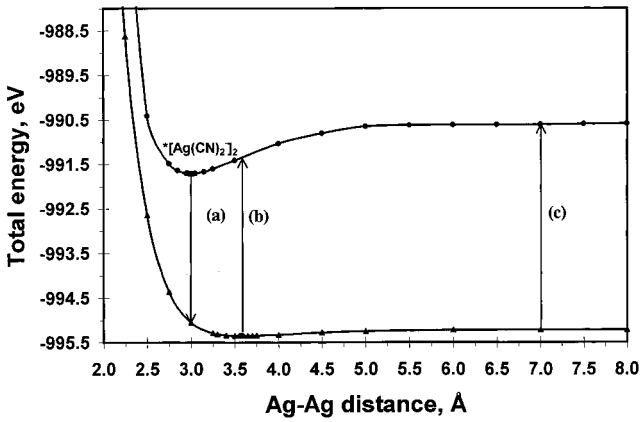

Figure 7. Excimer emission: Potential energy diagram of the ground and the excited state of $[Ag(CN)_2^-]_2$ (eclipsed configuration) plotted from extended Hückel calculations. The excimer $*[Ag(CN)_2^-]_2$ corresponds to the potential minimum of the excited state. Optical transitions shown are (a) excimer emission, (b) solid-state excitation, and (c) solution absorption.

characters of the HOMO and the LUMO orbitals. In both methods, the Ag orbital contribution of the HOMO and LUMO orbitals in the $[Ag(CN)_2^-]_2$ dimer consists of the same combination of atomic orbitals (the coefficients have the same sign but different values). Both calculation methods suggest that the HOMO is a σ antibonding orbital whereas the LUMO is a π bonding orbital with respect to Ag−Ag bonding. Given their qualitative similarity to the ab initio calculations, extended Hückel calculations have been used to study the excited states of the above models in order to reduce the calculation time.

Figure 7 shows a potential energy diagram for eclipsed $[Ag(CN)_2^-]_2$. The data are plotted from extended Hückel calculations for both the ground state and the first excited state to show the optical transitions. The ground state shows very little Ag−Ag bonding as indicated by its very shallow potential well. In contrast, significant Ag−Ag bonding is evident in the first excited state of the $[Ag(CN)_2^-]_2$ model. Table 2 summarizes the important results of ground- and excited-state calculations for $[Ag(CN)_2^-]_2$. The formation of a $*[Ag(CN)_2^-]_2$ excimer is indicated in Table 2 for the following reasons: (1) The Ag−Ag equilibrium distance is much shorter in the excited state than the ground state. The calculated excited state distortion of 0.58 A is very large and indicates that the nuclei undergo sizable rearrangement leading to their aggregation as a result of light absorption. (2) The potential well along the Ag−Ag bond is much deeper in the excited state than the ground state. This gives rise to a silver−silver-bonded excimer with a binding energy of 25.8 kcal/mol (1.12 eV). This value is about 9 times the corresponding value of the ground state in which silver−silver bonding is virtually not existing. (3) The Ag−Ag overlap population is greater in the excited state than in the ground state. The increase in the overlap population is more than 10 times greater in the $*[Ag(CN)_2^-]_2$ excimer than the ground-state dimer.

Table 2 shows that similar trends are obtained for the analogous staggered conformer. The staggered $*[Ag(CN)_2^-]_2$ excimer gives rise to a significantly shorter Ag−Ag distance, greater binding energy, and greater Ag−Ag overlap population than the corresponding $[Ag(CN)_2^-]_2$ ground-state dimer. A potential energy diagram similar to Figure 7 was obtained for the staggered dimer and is available in the Supporting Information. Table 2 shows that stronger Ag−Ag interactions exist in the staggered conformer than the eclipsed one. This is true for both the ground state (dimer) and the excited state (excimer). For instance, staggered $[Ag(CN)_2^-]_2$ has a Ag−Ag equilibrium distance that is 0.70 Å shorter than in the eclipsed conformer. On the other hand, the binding energy of the staggered excimer is 30.4 kcal/mol, or 4.6 kcal/mol greater than the corresponding value for the eclipsed excimer.

Table 2 shows that trimer models with different configurations yielded similar qualitative results to those obtained for the dimer models. For example, the staggered configuration of the linear trimer model gives rise to the formation of a $*[Ag(CN)_2^-]_3$ exciplex with a binding energy of 46.1 kcal/mol, a Ag−Ag distance of 2.46 Å (0.33 Å shorter than the ground-state trimer), and about twice the Ag−Ag binding energy of the ground-state trimer. The ground- and excited-state potential wells and relevant optical transitions for the staggered configuration of the linear trimer model are shown in Figure 8. Potential energy diagrams similar to Figures 7 and 8 have been obtained for the staggered dimer as well as for the eclipsed configurations of the linear and angular trimer models. These diagrams are available in the Supporting Information.

It should be emphasized that the magnitude of the shortening of the Ag−Ag distance (ΔQ) is presented in Table 2 in a qualitative sense, and therefore conclusions should not be drawn from the absolute values of these numbers. This is due to the low level of the calculations as well as the fact that these calculations are for free (undoped) $[Ag(CN)_2^-]_n$ species. Therefore, the actual ΔQ values for the different oligomers doped in the KCl lattice might be lower than the values shown in Table 2. Nevertheless, the KCl lattice can accommodate large excited-state distortions. For example, it has been reported that some color centers (F-centers) in KCl lattices have ΔQ values as large as 0.28 Å in crystals doped with Tl^+ ions.[44] Moreover, it has been reported that the emission in some KCl color centers occurs from the $\nu \sim 30$ excited state vibrational levels.[45]

4. Exciplex Tuning. The observation of different emission bands over such a broad range of wavelengths as shown in Figure 3 is quite unusual. This is especially true because these

(44) Markham, J. J. *F-Centers in Alkali Halides*; Academic Press: New York, 1966; p 382.

(45) Elliott, R. J.; Gibson, A. F. *An Introduction to Solid State Physics and its Applications*; Macmillan Press: London, 1976; p 192.

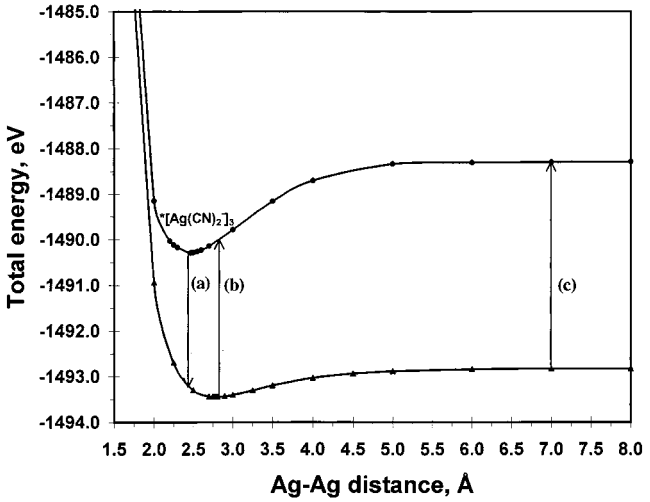

Figure 8. Exciplex emission: Potential energy diagram of the ground and the excited state of $[Ag(CN)_2^-]_3$ (staggered configuration) plotted from extended Hückel calculations. The exciplex $*[Ag(CN)_2^-]_3$ corresponds to the potential minimum of the excited state. Optical transitions shown are (a) exciplex emission, (b) solid-state excitation, and (c) solution absorption. Note the lower energies of transitions "a" and "b" relative to the corresponding transitions in Figure 7. Also note that the Ag−Ag distances are shorter and the potential wells are deeper than those in Figure 7 for both the ground state and excited state. See Table 2 for the specific values.

different emissions occur in a single crystal and the emission is tuned simply by changing the excitation wavelength. The emission bands in Figure 3 are assigned to various excimers and exciplexes formed in the studied crystals with a formula of $*[Ag(CN)_2^-]_n$. We call the new phenomenon *exciplex tuning* since the luminescence is *tuned* by the formation of different exciplexes. The luminescence energy depends on the identity of the $*[Ag(CN)_2^-]_n$ emissive exciplex.[37] Since the different exciplexes have different excitation bands one can tune the luminescence energy to a certain value by selecting the characteristic excitation wavelength of the exciplex responsible for this luminescence.

Figures 7 and 8 provide a nice illustration of the optical transitions observed in exciplex tuning. Solution absorption in these figures (transition "c") is depicted as a transition from the ground state to the excited state at a long Ag−Ag distance, at which no stabilization is present due to Ag−Ag interactions. This distance is arbitrarily chosen as 7.0 Å. This corresponds to the absorption spectrum of aqueous $Ag(CN)_2^-$ shown in Figure 5. Solid-state excitation is depicted as a transition from the ground state at a Ag−Ag distance corresponding to the minimum of the ground-state potential well (transition "b"). There is significant stabilization, especially in the excited state, due to Ag−Ag bonding. This stabilization explains the low energies of the excitation bands of the studied crystals (Figure 4) in comparison with the solution absorption band (Figure 5). Finally, the excimer/exciplex emission is depicted as a vertical transition from the minimum of the excited-state potential well to the ground state (transition "a"). These transitions correspond to the emission spectra shown in Figure 3. The extremely low energies of the excimer and exciplex emissions are due to a combined effect of excited-state stabilization and ground-state destabilization as clearly illustrated in Figures 7 and 8. The energy minimum in the excited state corresponds to a rather short Ag−Ag distance in the ground state at which the repulsive forces between the nuclei overwhelm the attractive forces between the nuclei and the electrons.

Table 3. Tentative Assignment of the Luminescence Bands of $Ag(CN)_2^-$/KCl at 77 K shown in Figures 3 and 4[a,46]

emission band	λ_{max}^{em}, nm	λ_{max}^{exc}, nm	assignment
A	285−300	225−240	$*[Ag(CN)_2^-]_2$ (excimers)
B	320−360	270−290	*cis*-$*[Ag(CN)_2^-]_3$ (localized exciplexes)
C	390−430	250−270	trans-$*[Ag(CN)_2^-]_3$ (localized exciplexes)
D	490−530	300−360	$*[Ag(CN)_2^-]_n$(delocalized exciplexes)

[a] In this paper we refer to an excited state dimer as an "excimer" while excited state trimers and longer oligomers are called "exciplexes".[37]

Figures 7 and 8 clearly show that the luminescence energies decrease significantly as one proceeds in the direction of monomer → dimer → trimer due to the formation of excimers and exciplexes. This provides the theoretical rationale behind the new exciplex tuning phenomenon. Experimentally, the shift to lower energies between the monomer and oligomers is illustrated by the energy difference between the solution absorption (Figure 5) and the solid-state excitation bands (Figure 4). Among the $[Ag(CN)_2^-]_n$ oligomers with the same configuration, the greater the value of "*n*" the lower the luminescence energy. Theoretically, this is indicated by a comparison of the luminescence energy depicted for the dimer (Figure 7) versus that for the trimer (Figure 8), and also by a comparison between the values of the HOMO−LUMO gap for the dimer and excimer versus those for the trimer and the corresponding $*[Ag(CN)_2^-]_3$ exciplex (Table 2). It should be pointed out that our ground-state extended Hückel calculations show that the trend continues as we proceed to the pentamer. The value of the HOMO−LUMO gap for the $[Ag(CN)_2^-]_5$ pentamer is smaller than the corresponding values for the dimer and trimer.

It is clear from the above discussion that the luminescence bands should decrease in energy as the number of interacting $Ag(CN)_2^-$ ions increase. Experimentally, the observation of several luminescence bands with distinctly different excitation and emission energies is consistent with these theoretical predictions. On this basis, we assign the luminescence bands in Figures 3 and 4 as due to the formation of $*[Ag(CN)_2^-]_n$ excimers and exciplexes with different values of "*n*". The assignment of all the luminescence bands is given in Table 3. Band A has the highest energy among all bands thus it corresponds to a small value of "*n*". Since "*n*" is ≥2, we assign band A to a $*[Ag(CN)_2^-]_2$ excimer. Since band D has the lowest energy among all bands observed in the KCl/$Ag(CN)_2^-$ crystals, we assign it to delocalized exciplexes. The fact that our calculations predict the formation of the pentanuclear $*[Ag(CN)_2^-]_5$ exciplex, which serves as a model for a delocalized exciplex, is consistent with this assignment. Bands B and C have intermediate energies between those of bands A and D and therefore they correspond to localized $*[Ag(CN)_2^-]_n$ exciplexes. A $*[Ag(CN)_2^-]_3$ trimer exciplex is a reasonable model for such localized exciplexes. The Ag atoms can be arranged in either a linear (*trans*-, $D_{\infty h}$) or an angular (*cis*-, C_{2v})-fashion in the trimer. Therefore bands B and C are assigned to angular and linear $*[Ag(CN)_2^-]_3$ trimer exciplexes, respectively.[46] The results of ground- and excited-state extended

(46) It is tempting to assign bands B and C to $*[Ag(CN)_2^-]_3$ and $*[Ag(CN)_2^-]_4$ trimer and tetramer exciplexes, respectively. However, we have reported recently that $Tl[Ag(CN)_2]$ has a luminescence band of the same energy as band C herein.[24] The crystal structure of $Tl[Ag(CN)_2]$ shows that the $Ag(CN)_2^-$ ions are arranged in trimer aggregations in which the Ag atoms are linear. Band C should therefore be assigned to a linear $*[Ag(CN)_2^-]_3$ trimer rather than a tetramer exciplex. An inspection of Figure 3 shows a band at ~470 nm. It is possible that this band represents the tetramer exciplex although the excitation spectrum of this band and that of band D are almost identical.

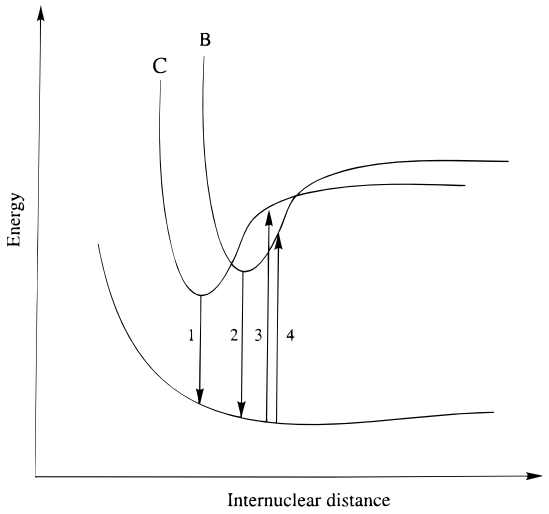

Figure 9. Potential surface model of the transitions responsible for bands B and C: 1, band C emission; 2, band B emission; 3, band C excitation; and 4, band B excitation. The energies of these transitions are consistent with the relative energies of bands B and C listed in Table 3.

Table 4. Lifetime Data for the Luminescence Bands of $Ag(CN)_2^-$/KCl at 77 K shown in Figure 3

emission band	lifetime, μs
A	4.8
B	3.1 (94%)
	16 (6%)
C	9.4 (54%)
	44 (46%)
D	5.2 (62%)
	20 (38%)

Hückel calculations for these trimer models support this assignment (Figure S5 in the Supporting Information).

Excited-state lifetimes for all luminescence bands are summarized in Table 4. The microsecond-level lifetimes indicate phosphorescence emission for all bands, i.e., the emissions occur from triplet $*[Ag(CN)_2^-]_n$ excimers and exciplexes. The observation of more than one microsecond component for bands B−D is consistent with the observation of other bands upon excitation with a wavelength characteristic of one particular band (Figure 3). The decay curve of band A, on the other hand, was fit with a single microsecond component, also in agreement with Figure 3 which shows virtually no other bands besides band A upon excitation with the characteristic wavelength of band A.

It is interesting to note that the excitation and emission maxima did not always follow the same trend. This is the case for bands B and C. While band C has a lower-energy emission maximum than band B, the excitation maximum was at a higher energy for band C (Figures 3 and 4, Table 3). This anomaly is explained by the model shown in Figure 9 which depicts the transitions responsible for bands B and C. This model is also consistent with the large overlap between bands B and C observed in the luminescence spectra. The observed larger Stokes shift for band C than band B is also accounted for in Figure 9 which shows that the potential surface of the excited state corresponding to band B is less-distorted than the one for band C.

Exciplex formation in the studied $Ag(CN)_2^-$/KCl crystals is supported by both the experimental and the theoretical results in this work. The experimental evidence includes the broadness of the luminescence bands, the absence of detailed structure in most emissions, the large Stokes shifts of the emission bands, and the very low luminescence energies. These are the typical features of the conventional excimer and exciplex emissions in organic compounds. In Figure 3, the full-width at half-maximum (fwhm) is ca. 3.32, 3.05, and 4.01×10^3 cm^{-1} for bands A, C, and D, respectively. The value of fwhm is not calculated for band B because there are two major components for this band, and we did not try to resolve them.[47] The high values of all these bandwidths are indicative of largely distorted excited states. Our theoretical calculations support this result as shown in Table 2 in which very large excited-state distortions are indicated by the significantly shorter Ag−Ag distances in the lowest excited states relative to the corresponding ground states.

The general absence of structure in the emission bands in Figure 3 is because the ground-state potential well is rather shallow in most cases and the emission transition terminates on the repulsive anharmonic part of the well. Figure 7 is most instructive of this point as the ground state is almost completely repulsive. Even when ground state Ag−Ag interactions become more significant as we go to trimers and pentamers, the emission is still expected to be structureless. The reason is because the excited state is largely distorted because the excimer or exciplex emissive state has a shorter Ag−Ag equilibrium distance than the ground state (Figures 7 and 8). The resulting emission ends up in the repulsive region away from the potential minimum of the ground state.

Large Stokes shifts are observed for the emission bands in Figure 3. The value of the Stokes shift, calculated as the energy difference between the emission peak and the corresponding excitation peak of the same band, is 7.7, 6.9, 14.5, and 13.3×10^3 cm^{-1} for bands A, B, C, and D, respectively. The large Stokes shifts of the emission bands shown in Figure 3 are explained by the large energy differences between the emission and the excitation transitions ("a" vs "b" in Figures 7 and 8). Note that the stabilization from the excited state is at its maximum for transition "a" while this stabilization is less for transition "b". Meanwhile, the ground state is actually stabilized for transition "b" (especially in Figure 8) but very highly destabilized for transition "a".

It is noted that the excitation spectra in Figure 4 are very highly unsymmetrical and structured. This is most likely due to the overlap between the different emissive states. Figure 4 shows that even when we carefully select the emission wavelength to minimize the contribution from other bands, a great deal of overlap still exists in the excitation spectra. The model shown in Figure 9 depicts the overlap between bands B and C. Some structure could be due to excitation to different vibrational levels of the excited state. However, the splitting between different peaks of the same band is not uniform. This could be due to the presence of a large anharmonicity factor. The largely distorted excited state is consistent with this possibility because this distortion implies excitation to the anharmonic region of the excited-state potential surface. However, we still rule out the significance of vibronic coupling for two reasons. First, if anharmonicity is involved then the spacing between different excitation peaks should decrease by proceeding to the higher energy (shorter wavelength) part of the structured band. This has not been observed. Second, this spacing does not correspond to any of the vibrational modes of $Ag(CN)_2^-$. For instance, the most prominent vibrational mode is the C−N symmetrical stretch (Figure 2) in the 2100 cm^{-1}

(47) In fact, even for bands A, C, and D, they are not perfectly symmetrical and they may be resolvable to more than one component. The values of fwhm indicated may not be accurate. Nevertheless, it is clear that all the bands are very broad.

region. Other vibrational modes include the Ag−C stretching and C−N bending modes in the 400 and 250 cm^{-1} regions, respectively.[24] The spacings between the structures in the excitation bands do not correspond to any of the aforementioned vibrational energies.

It is interesting to note that the emission bands in Figure 3 do not show the structured pattern observed in the excitation spectra shown in Figure 4. The overlap between the excitation bands is reflected in the emission spectra by the appearance of more than one band even when the excitation wavelength is selected to observe a certain band. For example, exciting with 315 nm in order to see band D has also resulted in band C emission, which appears as a shoulder. Also, exciting with 270 or 280 nm has not only resulted in emissions due to band B. Instead, bands C and D are also evident (Figure 3). A comparison between Figures 3 and 4 reveals that the emission bands are much more separated from each other than the excitation bands. This observation is explained by a careful inspection of Figures 7 and 8 which show that there is more difference among different exciplexes in the emission transition "a" than in the excitation transition "b". The difference in the binding energy between these exciplexes, as shown in Table 2, is responsible for this observation. Moreover, Table 2 shows that the differences in the HOMO−LUMO gaps between different exciplexes is greater than it is between the corresponding ground state aggregations.

Figure 3 shows that band B is resolved into two peaks. The prominent peak appears at ca. 327 and 345 nm for the spectra irradiated with 270 and 280 nm, respectively. Since the preceding discussion suggests that the factors affecting the structure of the excitation spectra have much less effect on the resolution of the emission spectra, a different reason is likely responsible for this structure. We assign the two peaks in band B to different geometrical isomers of the same type of exciplex. This assignment is also supported by our theoretical calculations. Table 2 shows that there is an appreciable difference between the eclipsed and the staggered conformers of the dimer and trimer models in both the ground state and the excited state. This difference is manifested by the different binding energies, HOMO−LUMO gaps, and Ag−Ag distances between the two species. The lower energies and shorter Ag−Ag distances in the staggered conformer are due to less steric interactions between the cyanide ligands in comparison to the eclipsed conformer. Table 2 also shows that the angular and linear structures of the eclipsed trimer attain significantly different results. These results emphasize that besides the length of the chain in the $[Ag(CN)_2^-]_n$ oligomers, the overall structure and the dihedral angle of a given oligomer also play a significant role in determining the luminescence energy. Therefore, a distribution analysis of the different oligomers and different geometrical isomers in the KCl lattice is worthwhile.

Table 5 shows the statistical distribution of the geometrical isomers of the $[Ag(CN)_2^-]_2$ dimer and the $[Ag(CN)_2^-]_3$ trimer. The fact that the dimers and trimers occupy significant percentages of the monomer sites (13% and 1.8%, respectively) indicates appreciable statistical probability for the oligomerization of $[Ag(CN)_2^-]_n$ species in the KCl lattice. Before drawing conclusions from the distribution analysis, one should consider the thermodynamic factors besides the statistical factors. For example, our recent MO calculations show that the total energy per $Ag(CN)_2^-$ ion decreases and the binding energy increases as one proceeds in the direction: monomer → dimer → trimer → pentamer.[20] This means that the probabilities for different oligomers deduced from the statistical distribution analysis provide the lower limit for the different oligomers, especially as the chain length increases.

Table 5. Statistical Distribution Analysis of the Geometrical Isomers of the $[Ag(CN)_2^-]_2$ Dimer and the $[Ag(CN)_2^-]_3$ Trimer in the KCl Lattice

species[a]	probability	% in studied crystal[b]	relative probability[c]
monomer	p	1.1	100
total dimer (D)	12 p^2	0.15	13
D1	($^{20}/_3$) p^2	0.081	7.3
D2	($^4/_3$) p^2	0.016	1.5
D3	4 p^2	0.048	4.4
total trimer (T)	150 p^3	0.020	1.8
T1	18 p^3	0.0024	0.22
T2	36 p^3	0.0048	0.44
T3	24 p^3	0.0032	0.29
T4	72 p^3	0.0096	0.87

[a] Notation: D1, perpendicular (C_{2v}) dimer; D2, eclipsed ($D_{\infty h}$) dimer; D3, offset-eclipsed (C_{2v}) dimer; T1, linear trimer ($D_{\infty h}$ for Ag atoms); T2, angular trimer, Ag atoms in the same plane (C_{2v}); T3, angular trimer, Ag atoms in different planes (C_{2v}); T4, triangular (D_{3h} for Ag atoms). See Charts 1 and 2. [b] Mole %. [c] Relative to the mole % of the monomer.

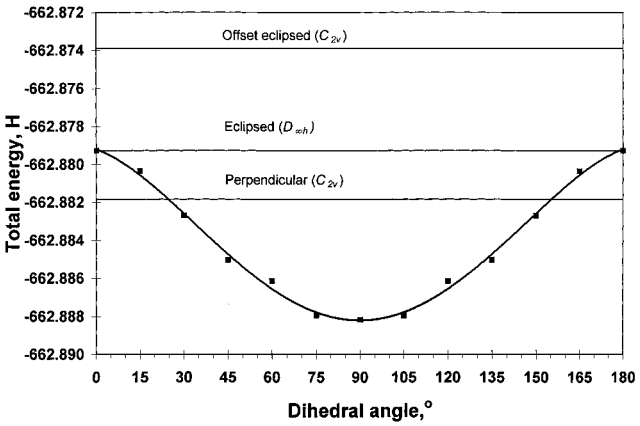

Figure 10. Total one-electron energy versus dihedral angle for $[Ag(CN)_2^-]_2$ as plotted from BECKE3LYP/LANL2DZ density functional calculations. The horizontal lines show the energies of the three possible configurations of the $[Ag(CN)_2^-]_2$ dimer in the KCl lattice (see Chart 1).

The thermodynamic factors should also be considered for the different geometrical isomers of a given oligomer. Figure 10 shows a plot of the total energy versus the dihedral angle for the $[Ag(CN)_2^-]_2$ dimer. It is obvious that the staggered dimer is the most thermodynamically favorable configuration with 5.58 kcal/mol lower energy than the eclipsed isomer. However, the staggered isomer cannot exist within the KCl lattice (see Chart 1). Among the three $[Ag(CN)_2^-]_2$ dimers that can exist in the KCl lattice, the perpendicular (C_{2v}) isomer has the lowest energy followed by the eclipsed ($D_{\infty h}$) and then the offset-eclipsed (C_{2v}) isomer. The fact that the energy of the offset-eclipsed (C_{2v}) isomer is much higher than the other two isomers indicates that this isomer may not exist in the KCl lattice. Therefore, although Table 5 shows that the statistical probability for the offset-eclipsed (C_{2v}) isomer is about 3 times that of the eclipsed ($D_{\infty h}$) isomer, the actual concentration of the $D_{\infty h}$ isomer is indeed more than the offset-eclipsed (C_{2v}) isomer (which may not exist at all). This is an important point because as one proceeds to longer oligomers, the number of geometrical isomers becomes very large. For example, the Ag backbone of the trimer has the four configurations shown in Chart 2. If one considers the isomers with the presence of the cyanide groups on the silver atoms, a total of 26 geometrical isomers are possible for the four structures shown in Chart 2. It is difficult to imagine that

Chart 2

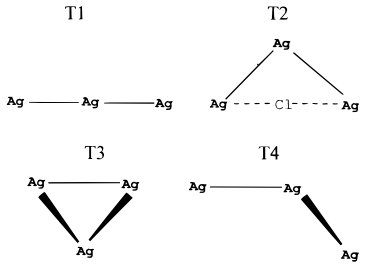

the number of peaks within the luminescence bands assigned to the trimer can be resolved to 26 peaks. Therefore, only a few of these isomers must be present in the KCl lattice.

Concluding Remarks

This study demonstrates remarkably rich luminescence properties for dicyanoargentate(I) systems. The new exciplex tuning phenomenon discovered in the $Ag(CN)_2^-$/KCl system reported herein illustrates unusual photophysical behavior of the dicyanoargentates(I). The formation of Ag−Ag-bonded excimers and exciplexes between adjacent $Ag(CN)_2^-$ ions in the KCl lattice gives rise to the different luminescence bands observed over the 285−610-nm range.[48] These species represent a new class of metal−metal-bonded inorganic exciplexes in which the bonding occurs between the same type of metal atoms. The tunability of the emission energy in the $Ag(CN)_2^-$/KCl system compares favorably with other systems that have been reported to display efficient tuning of their excited states. For example, Yersin and Gliemann have described the tunability of the luminescence energy in the tetracyanoplatinates (II).[39] However, to tune the emission over a large range of wavelengths, a combination of chemical substitution (changing the counterion) and application of high pressure must be applied in $[Pt(CN)_4]^{2-}$ systems. More recently, Cummings and Eisenberg have reported efficient tuning of the charge-transfer absorption and emission of Pt(diimine)(dithiolate) by 8160 and 7400 cm^{-1}, respectively.[38] Thirteen complexes were synthesized by varying the ligands to achieve this efficient tuning in the visible range. In exciplex tuning, on the other hand, the emission can be tuned by more than 18 000 cm^{-1} in the UV and visible ranges in a single crystal of $Ag(CN)_2^-$/KCl, simply by changing the excitation wavelength. This result is promising for potential applications of the $Ag(CN)_2^-$/KCl system.

Since the data in this study suggest that the interactions between dicyanoargentate (I) units occur predominantly in the lowest excited state, it is appropriate to present a comparison between ground-state versus excited-state metal−metal interactions. Unlike ground-state interactions, excited-state metal−metal interactions do not require very short metal−metal distances. Moreover, excited-state interactions are not very sensitive to the metal−metal distance. Instead, the number of interacting metal ions and their geometry play a central role in determining the extent of excited-state metal−metal interactions. For example, in $Tl[Ag(CN)_2]$, two emissive sites with quite different Ag−Ag distances showed emissions at the same energy.[24] One site has a short Ag−Ag distance (3.11 Å) and the other site has a much longer distance (3.53 Å) but the geometry of the two sites is similar. Also, Henary and Zink have noted that two isomers with similar ground-state Ag−Ag distances but different geometries showed quite different emission energies.[18] The silver atoms in the cube isomer of $Ag_4I_4(PPh_3)_4$ have more nearest-neighbor Ag atoms than the chair isomer. The emission energy was lower in the cube isomer than in the chair isomer despite the fact that the Ag−Ag distance is slightly longer in the former (3.12 Å) than in the latter (3.09 Å); thus, it was concluded that excited-state interactions play the dominant roles.[18] In contrast to the aforementioned systems with excited-state interactions, systems such as tetracyanoplatinates(II) which are well-known to have ground-state metal−metal interactions, show extreme sensitivity to the Pt−Pt distance in the ground state.[39]

Finally, this study sheds light into the exciplex phenomenon in inorganic versus organic systems. A well-known requirement for the observation of excimer-like emissions in conventional organic excimers in the solid state is that the interacting species must be stacked in layers.[49] We argue that the same requirement is valid for the formation of inorganic excimers and exciplexes. The only reported example of a coordination compound which forms metal−metal-bonded exciplexes in the solid state is $Tl[Ag(CN)_2]$.[24] The compound has a layered structure[20] and, therefore, satisfies this condition. Other $M[Ag(CN)_2]$ compounds (e.g., M = Na, K, $^1/_3K_2Na$, $^1/_2Ca$, $^1/_2Sr$) are also known to have layered structures[50] and recent results in our laboratory suggest that these compounds also show exciplex emissions.[51] The alkali halide host lattices allow the stacking of the $Ag(CN)_2^-$ dopant ions and thus it is not surprising to see exciplex emissions in these systems. Another aspect of the comparison between organic and inorganic exciplexes is ground-state interactions. It is generally known that such ground-state interactions are absent in conventional organic exciplexes. The present study indicates that this may not necessarily be the case in inorganic exciplexes as this study indicates the presence of ground-state Ag−Ag interactions.

Acknowledgment is made to the donors of the Petroleum Research Fund, administered by the American Chemical Society, for the support of this research. M.A.O. acknowledges an Academic Research Infrastructure Grant (No. 9512457) from the National Science Foundation and a grant from Paul J. Schupf for the Paul J. Schupf Scientific Computing Center at Colby College. We thank Professors Andrea Dorigo and Thomas Shattuck for their assistance with some calculations presented in this work. We also wish to thank Dr. Aleksander Siemiarczuk from the Fast Kinetics Application Laboratory at PTI for his help with the lifetime measurements.

Supporting Information Available: Figures of frontier orbitals and potential surfaces for both the ground and excited states of different $[Ag(CN)_2^-]_n$ aggregations (6 pages). See any current masthead page for ordering information and Internet access instructions.

JA980256T

(48) The limits of this range are based on wavelengths with intensities equal to or greater than the intensity at half-maximum for the luminescence bands in Figure 3.

(49) Ferguson, J. *J. Chem. Phys.* **1958**, *28*, 765. Stevens, B. *Spectrochim. Acta* **1962**, *18*, 439.

(50) (a) Range, K. J.; Kühnel, S.; Zabel, M. *Acta Crystallogr.* **1989**, *C45*, 1419. (b) Zabel, M.; Kühnel, S.; Range, K. J. *Acta Crystallogr.* **1989**, *C45*, 1619. (c) Hoard, J. L. *Z. Kristallogr.* **1933**, *84*, 231. Staritzky, E. *Anal. Chem.* **1956**, *28*, 419. (d) Range, K. J.; Zabel, M.; Meyer, H.; Fischer, H. *Z. Naturforsch.* **1985**, *40B*, 618. (e) Hoskins, B. F.; Robson, R.; Scarlett, N. V. Y. *J. Chem. Soc., Chem. Commun.* **1994**, 2025.

(51) Omary, M. A. Ph.D. Thesis, Graduate School, University of Maine, 1997.